THERMAL BARRIER COATING LIFE PREDICTION MODEL DEVELOPMENT*

R.V. Hillery, B.H. Pilsner, E.C. Duderstadt
General Electric
Aircraft Engine Business Group

The objectives of this program are to determine the predominant modes of degradation of a plasma sprayed thermal barrier coating system, and then to develop and verify life prediction models accounting for these degradation modes. The program is divided into two phases, each consisting of several tasks. The work in Phase I is aimed at identifying the relative importance of the various failure modes, and developing and verifying a life prediction model(s) for the predominant mode for a thermal barrier coating system. Two possible predominant failure mechanisms being evaluated are bond coat oxidation and bond coat creep. The work in Phase II will develop design-capable, causal, life prediction models for thermomechanical and thermochemical failure modes, and for the exceptional conditions of foreign object damage and erosion.

TBC SYSTEMS

The primary TBC system consists of a low pressure plasma-sprayed (LPPS) bond coat layer of Ni-22Cr-10Al-0.3Y, an air plasma sprayed yttria partially stabilized zirconia ($ZrO_2-8\%Y_2O_3$) top coat, on a conventionally cast Rene '80 substrate alloy (Table 1). This bond coat composition has been demonstrated to possess good oxidation resistance and has a large data base as a TBC bond coat. The $ZrO_2-8\%Y_2D_3$ top coat was chosen since numerous studies have shown that zirconia partially stabilized with 6-8 wt.% Y_2O_3 is the best composition for plasma sprayed TBC's (1). The Rene '80 substrate was chosen since a large TBC data base is present for this substrate composition.

Four different TBC systems utilizing four different bond coats are being evaluated in the experiment to evaluate the effect of bond coat creep strength on TBC thermal cycle life (Table 2). These four TBC systems also utilize $ZrO_2-8\%Y_2O_3$ top coats and Rene '80 substrates. TBC system #1 has the same NiCrAlY bond coat utilized in the primary TBC system. TBC systems #2, #3, and #4 have modified NiCrAlY bond coats which have received alloy additions to increase the bond coat creep strength. An aluminide overcoat is used in each of these systems (1-4) to reduce differences in oxidation resistance for the four bond coats. A comparison of the primary TBC system and its counterpart with an aluminide overcoat as the bond coat is shown in Figure 1.

THERMAL CYCLE TESTING

Thermal cycle testing is being performed in an automated Rapid Temperature Furnace (Figure 2). The thermal cycles consists of ten minutes heat up, a 45 minute exposure at 1093°C (2000°F), and 15 minutes forced air cooling. This furnace utilizes a lift which automatically cycles the specimens from the upper furnace exposure zone to the lower cooling compartment where a fan provides forced air cooling.

PRE-EXPOSURES IN AIR AND ARGON

In both the bond coat oxidation and bond coat creep evaluations, pre-exposures in air and argon have been utilized to evaluate the effect of bond coat oxidation on thermal cycle life. The specimens after each of the pre-exposure conditions (as-sprayed, argon, and air pre-exposures) are shown in Figure 3. The specimens pre-exposed in argon have top coats that are gray in appearance which can be attributed to oxygen deficiency, while the bond coat's silver color is indicative of the lack of significant oxidation. The specimens pre-exposed in air show that the bond coats have darkened due to oxidation, while the top coat's yellow appearance is typical of elevated temperature air exposure.

BOND COAT OXIDATION EXPERIMENT

In the bond coat oxidation experiment, pre-exposures in air and argon for different pre-exposure times were utilized. The goal of pre-exposures in air was to develop oxide scales prior to thermal cycling, while the goal of the pre-exposures in argon was to allow the other thermally activated phenomena present in the air pre-exposures to occur without developing the oxide scale. This should allow isolation of the effects of bond coat oxidation. Pre-exposures utilized were 10, 50, 100, and 500 hours both in air and argon. The oxide scale thicknesses of the air pre-exposures are plotted as a function of pre-exposure time in Figure 4.

Unexpectingly, the specimens pre-exposed in argon failed before the specimens pre-exposed in air (Figure 5). The initial hypothesis for this unexpected result is that a phase distribution change may be occurring in the ceramic top coat. Another surprising result was the longer lives for the specimens pre-exposed in air for 10 hours. The longer lives for these specimens than for the as-sprayed specimens may be due to bond coat sintering and perhaps top coat sintering. The sintering results in less constraint for the Al_2O_3 scale, while providing better top coat/bond coat adherence (improved chemical bonding).

Failure for these specimens was defined as when 10% (surface area) of the ceramic top coat has spalled (Figure 6). In all cases spalling initiated at the edges of the top coat. The failure location was the same for all pre-exposure conditions and occurred in the ceramic approximately 0.0025-0.0050 cm (0.001-0.002") from the bond coat/top coat interface.

Differences due to argon and air pre-exposures are clearly reflected in the pre-exposed, specimen microstructures (Figure 7). In all cases, a continuous Al_2O_3 film formed at the bond coat/top coat interface for specimens pre-exposed in air. The effect of oxidation is also seen in the bond coat microstructure where depletion of the high Al β phase is observed at the bond coat/top coat interface. The effect of interdiffusion in depletion of the high Al β phase in the bond coat is also observed at the bond coat substrate interface. The argon pre-exposures, on the other hand, significantly retarded bond coat oxidation. The effectiveness is demonstrated by the small degree of β depletion (high Al phase) in the bond coat at the bond coat/top coat interface and the absence of Al_2O_3 scale. These photomicrographs also show that significant interdiffusion that has occurred between the substrate and bond coat.

Differences due to argon and air pre-exposures are still reflected in the pre-exposed, specimen microstructure after thermal cycling. The microstructure of the specimen pre-exposed in argon after thermal cycling shows that very little β depletion has occurred in the bond coat at the bond coat/top coat interface. This is due to the argon pre-exposure and the short thermal cycle lives of these specimens (i.e. very little oxidation has occurred). This is contrasted with the microstructure of the specimens pre-exposed in air after thermal cycling where significantly more β depletion has occurred resulting in a larger ν layer at the bond coat/top coat interface. This illustrates the increased demand to continue the growth of the Al_2O_3 scale. Something that may be necessary to include in our model is the effect that a changing bond coat microstructure has on TBC integrity.

Oxide scale thickness measurements after thermal cycling indicate that bond coat oxidation may be a significant contribution to the failure mechanism. The oxide scale thickness after thermal cycling for the specimens pre-exposed in air and the specimens receiving no-pre-exposure are plotted in Figure 8. The plot shows that the oxide scale is essentially the same for the specimens regardless of pre-exposure time with the exception of the 500 hr. pre-exposure. This indicates that bond coat oxidation may be important. The 500 hr. pre-exposure result indicates this 4 μm oxide scale thickness is not large enough to cause failure if other thermally activated phenomena have not occurred. The oxide scales for the specimens pre-exposed in argon were less than 1 μm thick.

BOND COAT CREEP EFFECT EXPERIMENT

As mentioned previously, the bond coat creep effect experiment utilized four bond coats all of which had received aluminide over coats to reduce differences in oxidation resistance. Again, pre-exposures in air and argon were utilized (100 hr. pre-exposures). The results for air and argon pre-exposures again show that pre-exposures in argon are more detrimental than air pre-exposures (Figure 9). Also as expected, the TBC's with the NiCrAlY bond coat, which has the lowest bond coat creep strength, also had the lowest thermal cycle life. However, the separation between the other three bond coat creep systems is not clear. These results are also true for the specimens that received no pre-exposure (Figure 10). It is believed that the bond coat creep difference between these three particular systems (2, 3, 4) is not large enough to offset the effects of other contributions to failure. A new bond coat which has been developed at GE which has a creep strength lower than the three and closer to the bond coat creep strength of NiCrAlY will be used in future testing to demonstrate this effect more definitively.

KEY PROPERTY DETERMINATIONS

Key property determinations of the bond coat and the top coat will also be made in this study. The methods and conditions are listed in Figure 11. Generally, conventional testing can be utilized for the bond coat materials, whereas special testing is needed for the ceramic coatings.

TBC LIFE PREDICTION MODEL

The failure mechanism evaluations and key property determinations will then be coupled with thermomechanical studies to develop the life prediction models. Initial studies are aimed at determining the magnitude of strains present. The work will be done utilizing a tubular LCF bar, permitting internal cooling to develop thermal gradients (Figure 12). These initial studies will be used to set up a modified test matrix of experiments based on the initial studies to generate the thermomechanical data for the model.

1. Stecura, S. "Effects of Compositional Changes on the Performance of a Thermal Barrier Coating System," NASA TM 78976, 1979.

2. Miller, R.A., Garlick, R.G., and Smialek, J.L., "Phase Distributions in Plasma Sprayed Zirconia – Yttria," American Ceramic Society Bulletin, V.62, Dec. 1983, p. 1355-1358.

Table 1

Baseline Thermal Barrier Coating System
(Weight Percent)

- **Substrate (Rene'80):** Ni-14Cr-9. 5Co-5Ti-4W-4Mo-3Al-0.17C-0.3Zr-0.015B

- **Bond Coating:** Ni-22Cr-10Al-0.3Y (Low Pressure Plasma Spray)

- **Top Coating:** ZrO_2 - $8Y_2O_3$ (Air Plasma Spray)

Table 2
Bond Coat Creep Effect TBC Systems

Systems	Substrate/Bond Coating/Over Coating/Top Coating	Bond Coat Creep (Larson/Miller Parameter at 3 ksl — rupture test)
1	Rene'80/Bond Coating 1'/Aluminide/ ZrO_2-Y_2O_3	39.0
2	Rene'80/Bond Coating 2*/Aluminide/ ZrO_2-Y_2O_3	45.7
3	Rene'80/Bond Coating 3*/Aluminide/ ZrO_2-Y_2O_3	47.0
4	Rene'80/Bond Coating 4*/Aluminide/ ZrO_2-Y_2O_3	48.4

' NI-22Cr-10Al-0.3Y

* Modified NiCrAlY Bond Coats

As Sprayed TBC Microstructures
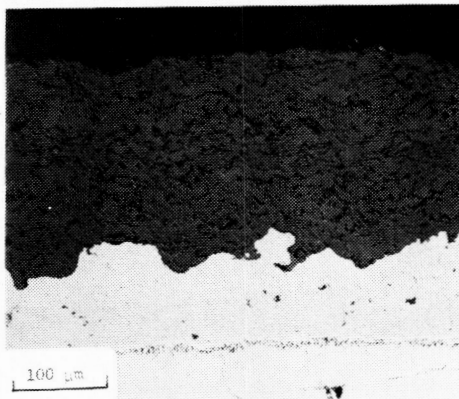
Rene'80/Ni-Cr-Al-Y/ZrO$_2$-Y$_2$O$_3$
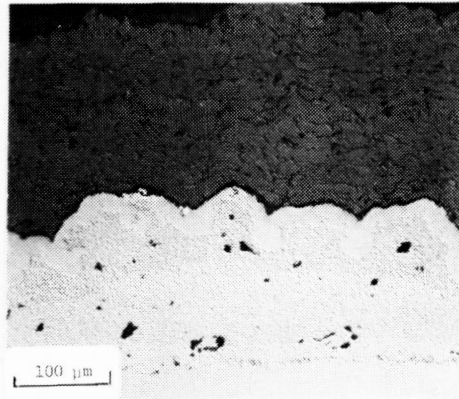
Rene'80/Ni-Cr-Al-Y/
Aluminide/ZrO$_2$-Y$_2$O$_3$

Figure 1   As-sprayed TBC microstructures

Figure 2   Rapid-temperature furnace

AS-SPRAYED

50 HRS. ARGON

50 HRS. AIR
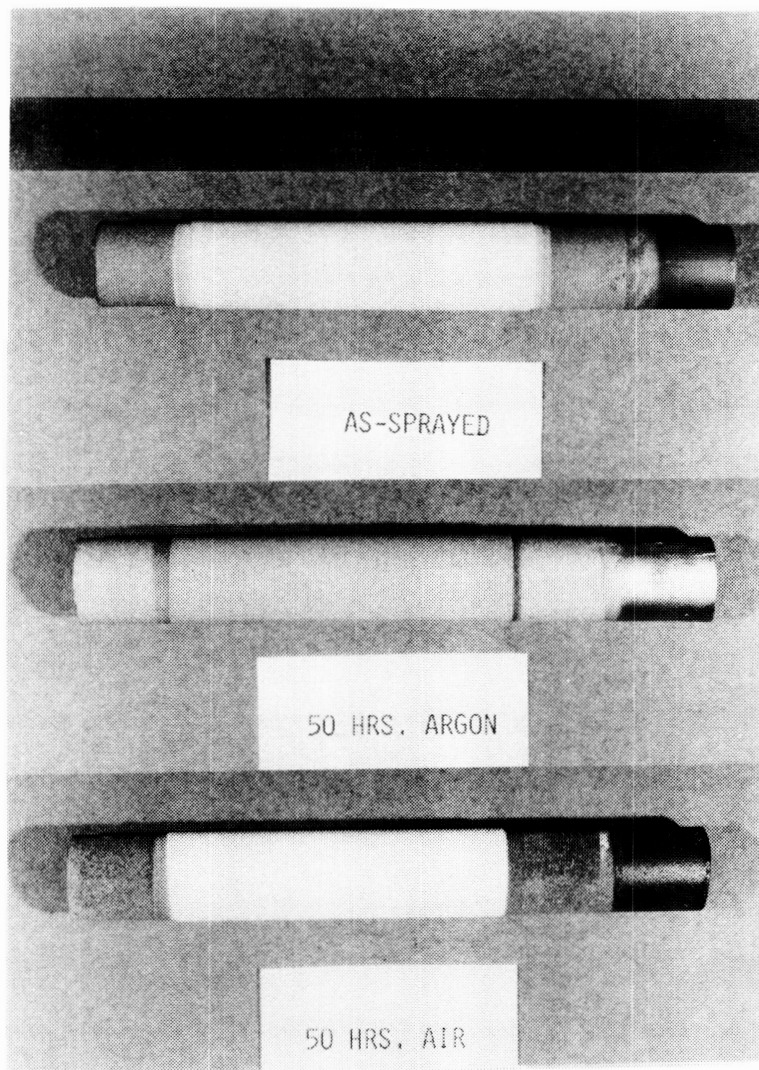
Figure 3 Specimens prior to thermal cycle testing

Oxidizing Pre-Exposure at 2000° F

Without Top Coat

With Top Coat

Oxide Scale
Thickness
(Microns)

Pre-Exposure Time — (Hours)
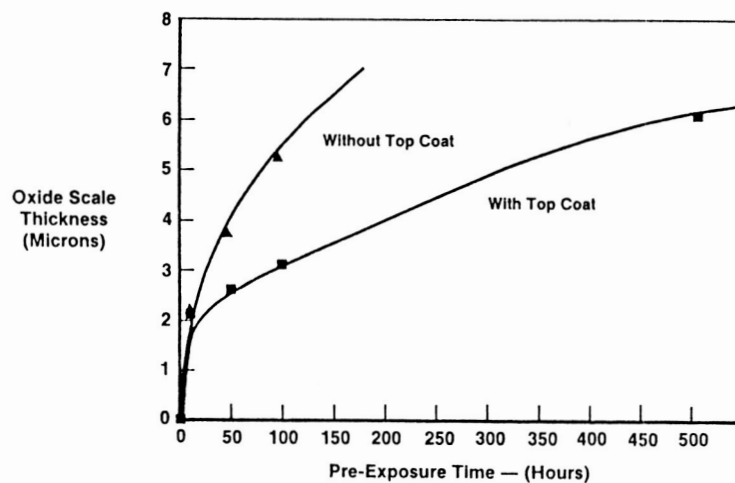
Figure 4

Rapid Temperature Thermal Cycle Test at 2000°F
45 Minute Exposure — 15 Minute Cool Down
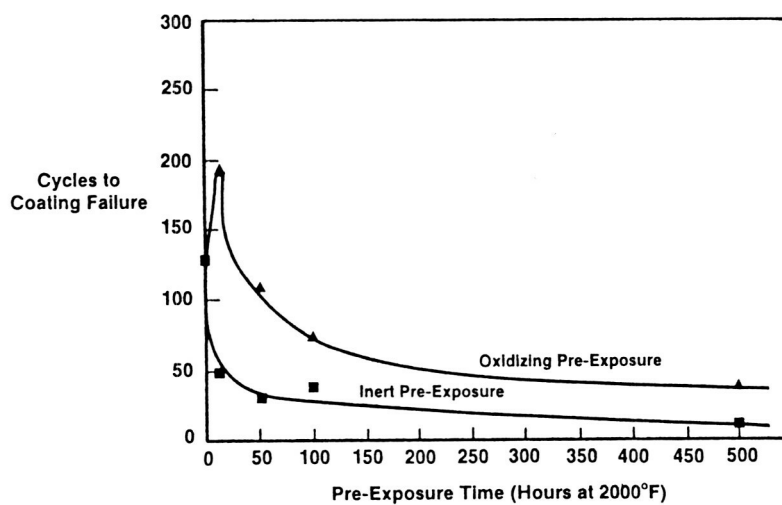
Figure 5
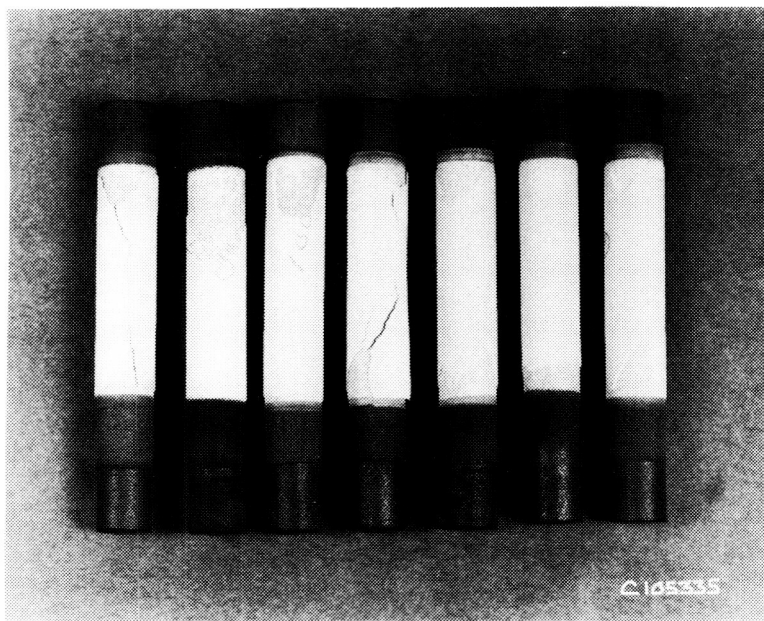
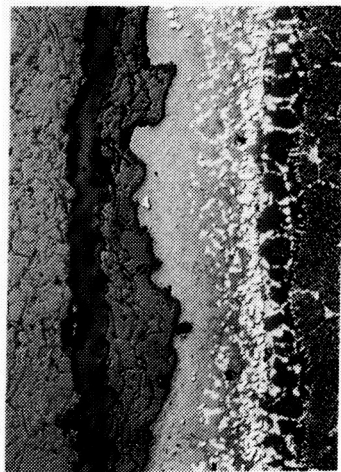Figure 6   Failed specimens after thermal cycle testing

NiCrAlY Bond Coat

100 Hour Air Pre-Exposure
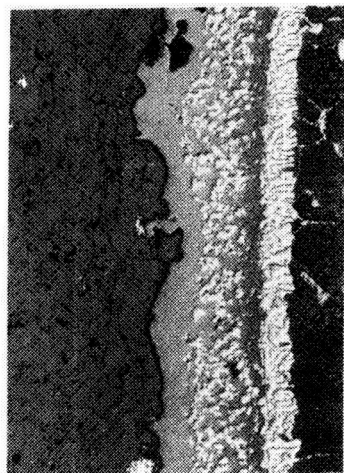
After Thermal Cycling

After Pre-Exposure

100 Hour Argon Pre-Exposure
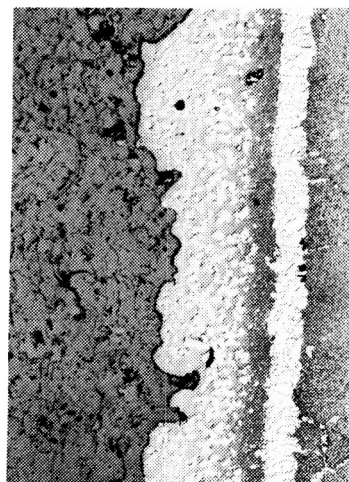
After Thermal Cycling

After Pre-Exposure

100 μm
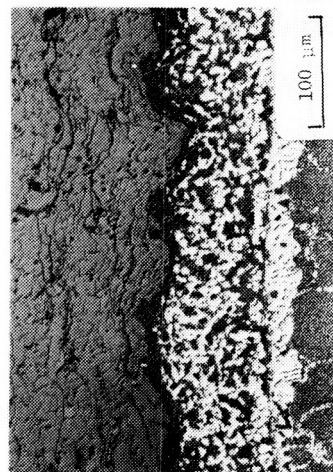
Figure 7

Al₂O₃ Scale Thickness at Failure
After Thermal Cycle Testing
(NiCrAlY Bond Coat)

Average Oxide Scale Thickness at Failure (Microns)

Thickness at Failure

Pre-Exposure Thickness

Pre-Exposure Time (Hours) →
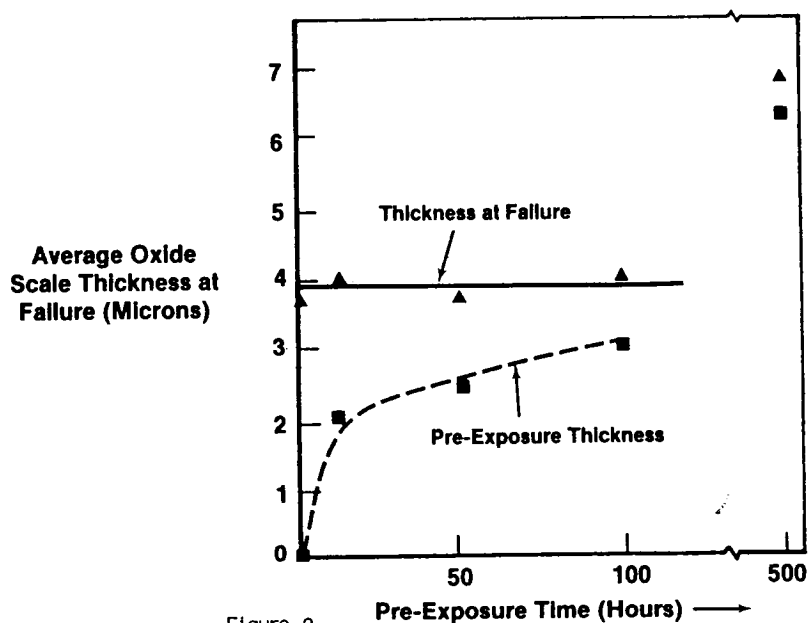
Figure 8

100 Hour Pre-Exposure

Cycles to Failure

Argon | Air

215 | 295 | 310 | 350 | 480 | 630 | 550 | 295

Argon | Air

1 Ni-22Cr-10Al-0.3Y
2,3,4 Modified NiCrAlY Bond Coats

Figure 9

As Sprayed

Cycles to Failure

1 NI-22Cr-10AI-0.3Y
2,3,4 Modified NICrAIY Bond Coats
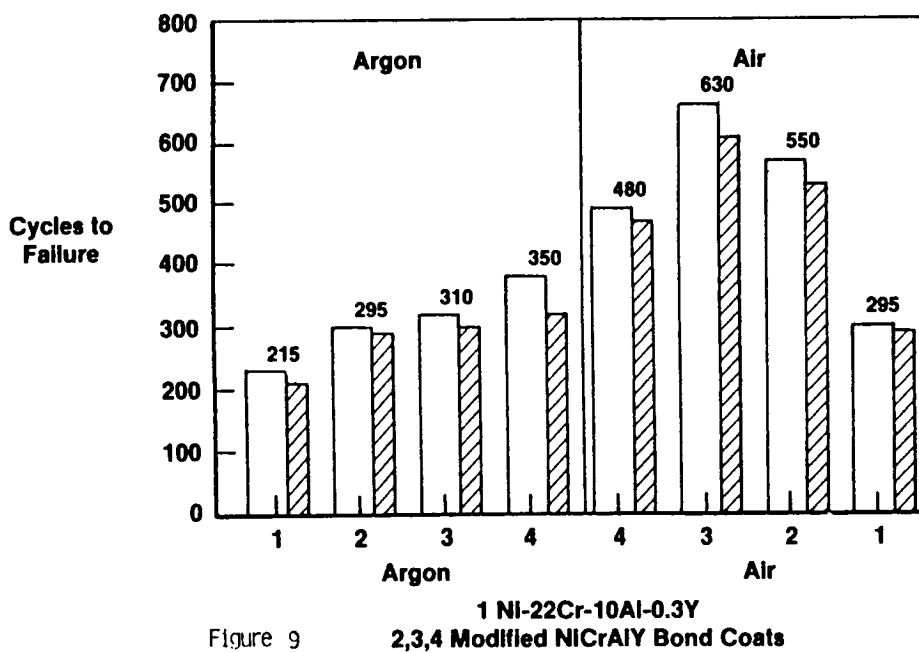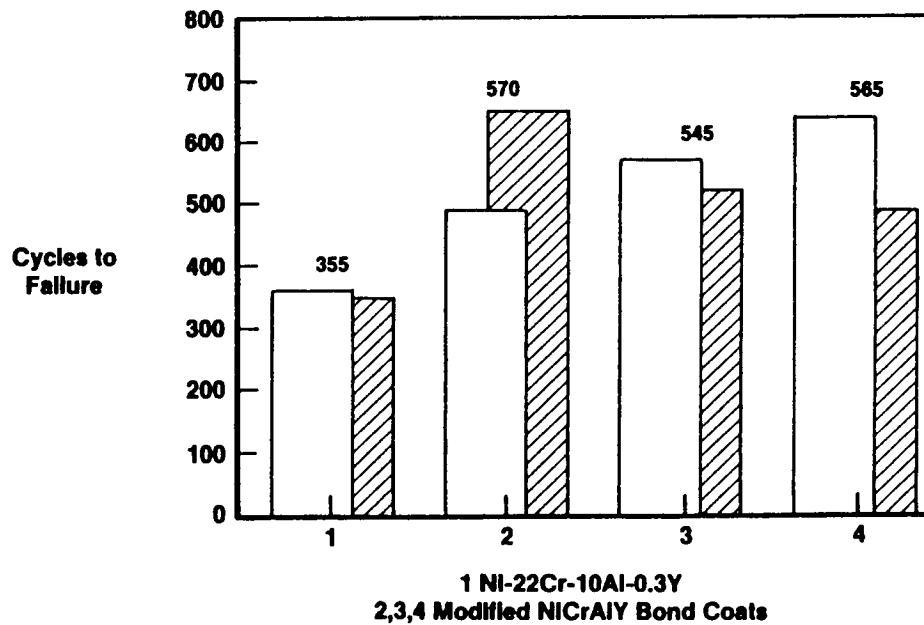
Figure 10

Key Mechanical Properties

	Bond Coating	Top Coating
● Tensile Strength	Conventional	Bend
● Poisson's Ratio	Conventional	Resonance*
● Coefficient of Thermal Exposure	Conventional	Conventional
● Dynamic Modulus	Conventional	Resonance
● Temperatures R.T., 1000°F, 1800°F, 1900°F, 2000°F		

*Also Strain Gauge at R.T.

Figure 11

Thermomechanical Properties
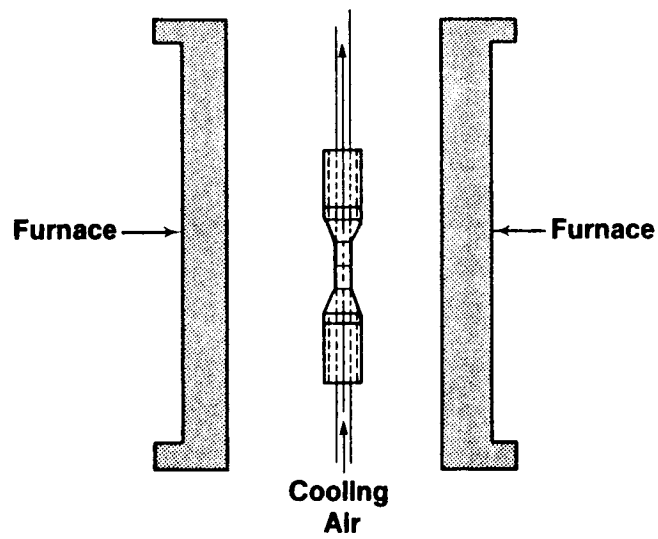
Determine Magnitude of Strains Present

Utilize Test Matrix of LCF Testing

Figure 12